Research Article | Vol. 25, No. 4 | 20 Feb 2017 | OPTICS EXPRESS 3411

Optics EXPRESS

Anisotropic dependence of tune-out wavelength near Dy 741-nm transition

WIL KAO,[1,2] YIJUN TANG,[2,3,*] NATHANIEL Q. BURDICK,[1,2] AND BENJAMIN L. LEV[1,2,3]

[1]*Department of Applied Physics, Stanford University, Stanford, California 94305, USA*
[2]*E. L. Ginzton Laboratory, Stanford University, Stanford, California 94305, USA*
[3]*Department of Physics, Stanford University, Stanford, California 94305, USA*
[*] *yijun2@stanford.edu*

Abstract: We report the first measurement of a tune-out wavelength for ground-state bosonic Dy and linearly polarized light. The tune-out wavelength is measured as a detuning from the nearby narrow-line 741-nm transition in ^{162}Dy, and is the wavelength at which the total Stark shift of the ground state vanishes. We find that it strongly depends on the relative angle between the optical field and quantization axis due to Dy's large tensor polarizability. This anisotropy provides a wide, 22-GHz tunability of the tune-out frequency for linearly polarized light, in contrast to Rb and Cs whose near-infrared tune-out wavelengths do not exhibit large anisotropy. The measurements of the total light shift are performed by measuring the contrast of multipulse Kapitza-Dirac diffraction. The calculated wavelengths are within a few GHz of the measured values using known Dy electronic transition data. The lack of hyperfine structure in bosonic Dy implies that the tune-out wavelengths for the other bosonic Dy isotopes should be related to this ^{162}Dy measurement by the known isotope shifts.

OCIS codes: (020.1475) Bose-Einstein condensates; (020.6580) Stark effect

References and links

1. C. C. Bradley, J. J. McClelland, W. R. Anderson, and R. J. Celotta, "Magneto-optical trapping of chromium atoms," Phys. Rev. A **61**, 053407 (2000).
2. J. J. McClelland and J. L. Hanssen, "Laser Cooling without Repumping: A Magneto-Optical Trap for Erbium Atoms," Phys. Rev. Lett. **96**, 143005 (2006).
3. M. Lu, S. H. Youn, and B. L. Lev, "Trapping Ultracold Dysprosium: A Highly Magnetic Gas for Dipolar Physics," Phys. Rev. Lett. **104**, 063001 (2010).
4. S. H. Youn, M. Lu, U. Ray, and B. L. Lev, "Dysprosium magneto-optical traps," Phys. Rev. A **82**, 043425 (2010).
5. D. Sukachev, A. Sokolov, K. Chebakov, A. Akimov, S. Kanorsky, N. Kolachevsky, and V. Sorokin, "Magneto-optical trap for thulium atoms," Phys. Rev. A **82**, 011405 (2010).
6. J. Miao, J. Hostetter, G. Stratis, and M. Saffman, "Magneto-optical trapping of holmium atoms," Phys. Rev. A **89**, 041401 (2014).
7. A. Griesmaier, J. Werner, S. Hensler, J. Stuhler, and T. Pfau, "Bose-Einstein Condensation of Chromium," Phys. Rev. Lett. **94**, 160401 (2005).
8. M. Lu, N. Q. Burdick, S. H. Youn, and B. L. Lev, "Strongly Dipolar Bose-Einstein Condensate of Dysprosium," Phys. Rev. Lett. **107**, 190401 (2011).
9. M. Lu, N. Q. Burdick, and B. L. Lev, "Quantum degenerate dipolar Fermi gas," Phys. Rev. Lett. **108**, 215301 (2012).
10. K. Aikawa, A. Frisch, M. Mark, S. Baier, A. Rietzler, R. Grimm, and F. Ferlaino, "Bose-Einstein Condensation of Erbium," Phys. Rev. Lett. **108**, 210401 (2012).
11. K. Aikawa, A. Frisch, M. Mark, S. Baier, R. Grimm, and F. Ferlaino, "Reaching Fermi degeneracy via universal dipolar scattering," Phys. Rev. Lett. **112**, 010404 (2014).
12. Y. Tang, N. Q. Burdick, K. Baumann, and B. L. Lev, "Bose-Einstein condensation of ^{162}Dy and ^{160}Dy," New J. Phys. **17**, 045006 (2015).
13. B. Naylor, A. Reigue, E. Maréchal, O. Gorceix, B. Laburthe-Tolra, and L. Vernac, "Chromium dipolar Fermi sea," Phys. Rev. A **91**, 011603 (2015).
14. S. R. Manmana, E. M. Stoudenmire, K. R. A. Hazzard, A. M. Rey, and A. V. Gorshkov, "Topological phases in ultracold polar-molecule quantum magnets," Phys. Rev. B **87**, 081106 (2013).
15. T.-S. Zeng and L. Yin, "Fractional quantum Hall states of dipolar gases in Chern bands," Phys. Rev. B **91**, 075102 (2015).
16. D. Peter, N. Y. Yao, N. Lang, S. D. Huber, M. D. Lukin, and H. P. Büchler, "Topological bands with a Chern number $C = 2$ by dipolar exchange interactions," Phys. Rev. A **91**, 053617 (2015).

#282926 https://doi.org/10.1364/OE.25.003411
Journal © 2017 Received 15 Dec 2016; accepted 28 Jan 2017; published 8 Feb 2017

Optics EXPRESS

17. N. Y. Yao, S. D. Bennett, C. R. Laumann, B. L. Lev, and A. V. Gorshkov, "Bilayer fractional quantum Hall states with dipoles," Phys. Rev. A **92**, 033609 (2015).
18. S. Baier, M. J. Mark, D. Petter, K. Aikawa, L. Chomaz, Z. Cai, M. Baranov, P. Zoller, and F. Ferlaino, "Extended Bose-Hubbard models with ultracold magnetic atoms," Science **352**, 201 (2016).
19. H. Kadau, M. Schmitt, M. Wenzel, C. Wink, T. Maier, I. Ferrier-Barbut, and T. Pfau, "Observing the Rosensweig instability of a quantum ferrofluid," Nature **530**, 194–197 (2016).
20. F. Wächtler and L. Santos, "Quantum filaments in dipolar Bose-Einstein condensates," Phys. Rev. A **93**, 061603 (2016).
21. D. Baillie, R. M. Wilson, R. N. Bisset, and P. B. Blakie, "Self-bound dipolar droplet: A localized matter wave in free space," Phys. Rev. A **94**, 021602 (2016).
22. I. Ferrier-Barbut, H. Kadau, M. Schmitt, M. Wenzel, and T. Pfau, "Observation of Quantum Droplets in a Strongly Dipolar Bose Gas," Phys. Rev. Lett. **116**, 215301 (2016).
23. L. Chomaz, S. Baier, D. Petter, M. J. Mark, F. Wächtler, L. Santos, and F. Ferlaino, "Quantum-fluctuation-driven crossover from a dilute Bose-Einstein condensate to a macro-droplet in a dipolar quantum fluid," Phys. Rev. X **6**, 041039 (2016).
24. M. Schmitt, M. Wenzel, F. Böttcher, I. Ferrier-Barbut, and T. Pfau, "Self-bound droplets of a dilute magnetic quantum liquid," Nature **539**, 259–262 (2016).
25. R. Grimm, M. Weidemüller, and Y. B. Ovchinnikov, "Optical Dipole Traps for Neutral Atoms," in *Advances In Atomic, Molecular, and Optical Physics*, Vol. 42, (Elsevier, 2000), pp. 95–170.
26. L. J. LeBlanc and J. H. Thywissen, "Species-specific optical lattices," Phys. Rev. A **75**, 053612 (2007).
27. B. Arora, M. S. Safronova, and C. W. Clark, "Tune-out wavelengths of alkali-metal atoms and their applications," Phys. Rev. A **84**, 043401 (2011).
28. Y. Cheng, J. Jiang, and J. Mitroy, "Tune-out wavelengths for the alkaline-earth-metal atoms," Phys. Rev. A **88**, 022511 (2013).
29. U. Dammalapati, K. Harada, and Y. Sakemi, "Magic and tune-out wavelengths for atomic francium," Phys. Rev. A **93**, 043407 (2016).
30. C. D. Herold, V. D. Vaidya, X. Li, S. L. Rolston, J. V. Porto, and M. S. Safronova, "Precision measurement of transition matrix elements via light shift cancellation," Phys. Rev. Lett. **109**, 243003 (2012).
31. B. M. Henson, R. I. Khakimov, R. G. Dall, K. G. H. Baldwin, L.-Y. Tang, and A. G. Truscott, "Precision Measurement for Metastable Helium Atoms of the 413 nm Tune-Out Wavelength at Which the Atomic Polarizability Vanishes," Phys. Rev. Lett. **115**, 043004 (2015).
32. L. W. Clark, L.-C. Ha, C.-Y. Xu, and C. Chin, "Quantum Dynamics with Spatiotemporal Control of Interactions in a Stable Bose-Einstein Condensate," Phys. Rev. Lett. **115**, 155301 (2015).
33. R. H. Leonard, A. J. Fallon, C. A. Sackett, and M. S. Safronova, "High-precision measurements of the ^{87}Rb D-line tune-out wavelength," Phys. Rev. A **92**, 052501 (2015).
34. F. Schmidt, D. Mayer, M. Hohmann, T. Lausch, F. Kindermann, and A. Widera, "Precision measurement of the ^{87}Rb tune-out wavelength in the hyperfine ground state $F = 1$ at 790 nm," Phys. Rev. A **93**, 022507 (2016).
35. J. Catani, G. Barontini, G. Lamporesi, F. Rabatti, G. Thalhammer, F. Minardi, S. Stringari, and M. Inguscio, "Entropy Exchange in a Mixture of Ultracold Atoms," Phys. Rev. Lett. **103**, 140401 (2009).
36. D. C. McKay, C. Meldgin, D. Chen, and B. DeMarco, "Slow Thermalization between a Lattice and Free Bose Gas," Phys. Rev. Lett. **111**, 063002 (2013).
37. T. Topcu and A. Derevianko, "Tune-out wavelengths and landscape-modulated polarizabilities of alkali-metal Rydberg atoms in infrared optical lattices," Phys. Rev. A **88**, 053406 (2013).
38. V. D. Vaidya, J. Tiamsuphat, S. L. Rolston, and J. V. Porto, "Degenerate Bose-Fermi mixtures of rubidium and ytterbium," Phys. Rev. A **92**, 043604 (2015).
39. A. Griessner, A. J. Daley, S. R. Clark, D. Jaksch, and P. Zoller, "Dark-State Cooling of Atoms by Superfluid Immersion," Phys. Rev. Lett. **97**, 220403 (2006).
40. M. Krämer, L. Pitaevskii, and S. Stringari, "Macroscopic Dynamics of a Trapped Bose-Einstein Condensate in the Presence of 1D and 2D Optical Lattices," Phys. Rev. Lett. **88**, 180404 (2002).
41. H. Pu, L. O. Baksmaty, W. Zhang, N. P. Bigelow, and P. Meystre, "Effective-mass analysis of Bose-Einstein condensates in optical lattices: Stabilization and levitation," Phys. Rev. A **67**, 043605 (2003).
42. H. Ott, E. de Mirandes, F. Ferlaino, G. Roati, G. Modugno, and M. Inguscio, "Collisionally Induced Transport in Periodic Potentials," Phys. Rev. Lett. **92**, 160601 (2004).
43. M. Bruderer, T. H. Johnson, S. R. Clark, D. Jaksch, A. Posazhennikova, and W. Belzig, "Phonon resonances in atomic currents through Bose-Fermi mixtures in optical lattices," Phys. Rev. A **82**, 043617 (2010).
44. D. M. Bauer, M. Lettner, C. Vo, G. Rempe, and S. Dürr, "Combination of a magnetic Feshbach resonance and an optical bound-to-bound transition," Phys. Rev. A **79**, 062713 (2009).
45. M. Yan, B. J. DeSalvo, B. Ramachandhran, H. Pu, and T. C. Killian, "Controlling Condensate Collapse and Expansion with an Optical Feshbach Resonance," Phys. Rev. Lett. **110**, 123201 (2013).
46. Z. Fu, P. Wang, L. Huang, Z. Meng, H. Hu, and J. Zhang, "Optical control of a magnetic Feshbach resonance in an ultracold Fermi gas," Phys. Rev. A **88**, 041601 (2013).
47. V. A. Dzuba, V. V. Flambaum, and B. L. Lev, "Dynamic polarizabilities and magic wavelengths for dysprosium," Phys. Rev. A **83**, 032502 (2011).

Optics EXPRESS

48. H. Li, J.-F. Wyart, O. Dulieu, S. Nascimbène, and M. Lepers, "Optical trapping of ultracold dysprosium atoms: transition probabilities, dynamic dipole polarizabilities and van der Waals C_6 coefficients," J. Phys. B **50**, 014005 (2017).
49. M. Lepers, J.-F. Wyart, and O. Dulieu, "Anisotropic optical trapping of ultracold erbium atoms," Phys. Rev. A **89**, 022505 (2014).
50. Y. J. Lin, R. L. Compton, K. Jiménez-García, J. V. Porto, and I. B. Spielman, "Synthetic magnetic fields for ultracold neutral atoms," Nature **462**, 628–632 (2009).
51. Y. J. Lin, K. Jiménez-García, and I. B. Spielman, "Spin-orbit-coupled Bose-Einstein condensates," Nature **471**, 83–86 (2011).
52. N. Q. Burdick, Y. Tang, and B. L. Lev, "Long-lived spin-orbit-coupled degenerate dipolar Fermi gas," Phys. Rev. X **6**, 031022 (2016).
53. P. L. Kapitza and P. A. M. Dirac, "The reflection of electrons from standing light waves," Math. Proc. Cambridge Philos. Soc. **29**, 297–300 (1933).
54. G. Birkl, M. Gatzke, I. H. Deutsch, S. L. Rolston, and W. D. Phillips, "Bragg scattering from atoms in optical lattices," Phys. Rev. Lett. **75**, 2823–2826 (1995).
55. G.-B. Jo, J. Guzman, C. K. Thomas, P. Hosur, A. Vishwanath, and D. M. Stamper-Kurn, "Ultracold Atoms in a Tunable Optical Kagome Lattice," Phys. Rev. Lett. **108**, 045305 (2012).
56. P. Cheiney, C. M. Fabre, F. Vermersch, G. L. Gattobigio, R. Mathevet, T. Lahaye, and D. Guéry-Odelin, "Matter-wave scattering on an amplitude-modulated optical lattice," Phys. Rev. A **87**, 013623 (2013).
57. B. Gadway, D. Pertot, R. Reimann, M. G. Cohen, and D. Schneble, "Analysis of Kapitza-Dirac diffraction patterns beyond the Raman-Nath regime," Opt. Express **17**, 19173–19180 (2009).
58. K. Baumann, N. Q. Burdick, M. Lu, and B. L. Lev, "Observation of low-field Fano-Feshbach resonances in ultracold gases of dysprosium," Phys. Rev. A **89**, 020701 (2014).
59. M. Lu, S. H. Youn, and B. L. Lev, "Spectroscopy of a narrow-line laser-cooling transition in atomic dysprosium," Phys. Rev. A **83**, 012510 (2011).
60. I. H. Deutsch and P. S. Jessen, "Quantum-state control in optical lattices," Phys. Rev. A **57**, 1972–1986 (1998).
61. J. M. Geremia, J. K. Stockton, and H. Mabuchi, "Tensor polarizability and dispersive quantum measurement of multilevel atoms," Phys. Rev. A **73**, 042112 (2006).
62. J. Mitroy, M. S. Safronova, and C. W. Clark, "Theory and applications of atomic and ionic polarizabilities," J. Phys. B: At. Mol. Opt. Phys. **43**, 202001 (2010).
63. D. A. Steck, "Quantum and Atom Optics," http://steck.us/teaching (revision 0.11.0, 18 August 2016).
64. L. Ma, J. Indergaard, B. Zhang, I. Larkin, R. Moro, and W. A. de Heer, "Measured atomic ground-state polarizabilities of 35 metallic elements," Phys. Rev. A **91**, 010501 (2015).

1. Introduction

The recent trapping and laser cooling of magnetic dipolar atomic elements such as chromium [1], erbium [2], dysprosium [3, 4], thulium [5], and holmium [6], with the first three having been cooled to quantum degeneracy [7–13], has opened new avenues of ultracold atomic physics exploration. Specifically, the long-range and anisotropic character of the magnetic dipole-dipole interaction provides a platform to investigate the role dipolar physics can play in quantum simulation. Examples of the latter include proposals to realize topologically non-trivial systems [14–17], and recent progress includes the study of the extended Bose-Hubbard model using erbium [18] and the observation of the arrested implosion of a dipolar dysprosium BEC due to the balance between the mean-field potential and quantum fluctuations [19–24].

Neutral atoms experience a force in an inhomogeneous light field. The resulting trapping force arises from the interaction between the light field and the induced atomic dipole moment and leads to the so-called Stark shift in the atomic energy level [25]. The total Stark shift can vanish at certain wavelengths due to cancellation between multiple atomic transitions. Such "tune-out" wavelengths for various atomic species have been predicted theoretically [26–29] and measured experimentally [30–34]. This knowledge is particularly useful for engineering species-specific trapping potentials. For example, in mixed-species experiments, one can create an optical lattice potential for one species but not the other [35–38], and the interaction between the trapped species and the background species allows for the implementation of novel cooling schemes to realize new quantum phases [39]. This species-specific lattice can also be used to tune the interspecies effective mass ratio of the trapped atoms [26], allowing for the flexible exploration of collective dynamics [40, 41]. Lastly, the coexistence of trapped fermions and a background

Optics EXPRESS

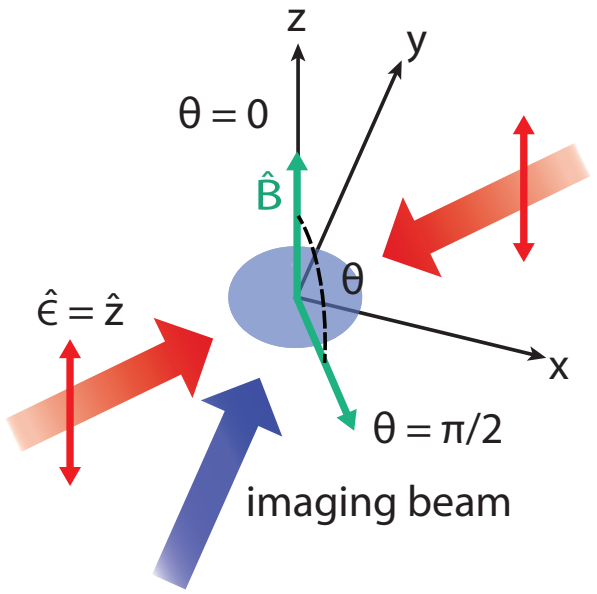

Fig. 1. Schematic of lattice beam (red arrow; with polarization $\hat{\epsilon}$) geometry used to measure lattice depth by KD diffraction of the BEC (blue sphere). Green arrows indicate direction of the applied magnetic field.

bosonic gas can potentially simulate phonon-like excitations in an optical lattice [26, 42, 43].

Aside from engineering trapping potentials for neutral atoms, knowledge of tune-out wavelengths is also useful in the context of the optical control of Feshbach resonances (OFR), a promising technique to achieve time-varying and/or spatially modulated interatomic interactions [32, 44–46]. One can operate the OFR laser at a far-off-resonance regime to reduce heating and loss rate and, if possible, at the tune-out wavelength of the targeted atomic species so that the parasitic dipole force of the OFR beam is eliminated, as recently demonstrated by [32]. The longer lifetime permits studies of the non-equilibrium dynamics of quantum gases with long observation times when the tune-out wavelength is far-detuned from electronic transitions [32].

The precise determination of atomic transition strengths cannot rest on *ab initio* quantum-mechanical calculations alone due to the electronic complexity of lanthanides like dysprosium, the atom considered here. The complicated electronic structure of these open-f-shell lanthanide elements presents a significant challenge for such analyses (see [47] and the recent study [48]) and experimental investigations are crucial for understanding their electronic structure. For example, in [49], a semi-empirical approach that utilizes both theoretical calculations and experimental data leads to the prediction of nine unobserved odd-parity energy levels in the erbium atomic spectrum. More generally, improved knowledge of atomic polarizabilities, which are informed by measurements of tune-out wavelengths [34], can guide choices of, e.g., optical dipole trapping wavelengths and laser wavelengths for implementing Raman transitions for realizing synthetic gauge fields [50–52]. It is in this spirit that we present the measurement of the tune-out wavelength for the bosonic ^{162}Dy near the narrow 741-nm transition.

We proceed by describing the experimental system in Sec. 2 before introducing the calculation of Stark shifts in Sec. 3 and results of our measurements in Sec. 4.

Optics EXPRESS

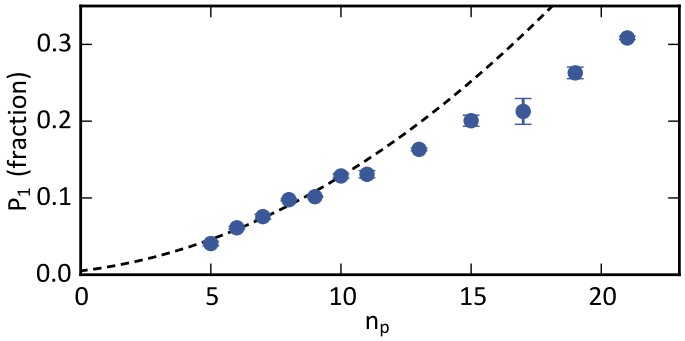

Fig. 2. Fractional first-order diffracted population at a constant laser power and wavelength. Each point is an average of three measurements shown with 1σ standard error. For optimal SNR, we use the maximum pulse number up to which the quadratic enhancement holds (i.e., $n_p = 10$). The first six data points are fit to Eq. (1). The dashed line is the resulting fit, which yields a measured lattice depth of $U_0 = 0.20E_R$.

2. Experimental methods

Using linearly polarized light, we probe the total (scalar plus tensor) light shift in the vicinity of the 741-nm transition by Kapitza-Dirac (KD) lattice diffraction [53], which is a standard tool for optical lattice characterization [54–56]. See Fig. 1. The vector light shift vanishes for linearly polarized light. See Sec. 3. The lattice depth U_0 is measured in units of recoil energy $E_r = (\hbar k_r)^2/2m$, where m is the mass of the atom, $k_r = 2\pi/\lambda$ is the grating wavevector, and λ is the wavelength of the laser.

We perform KD diffraction such that $\omega_r t \gtrsim 1$, where the recoil angular frequency is $\omega_r = E_r/\hbar$ and the grating pulse length t is sufficiently long to induce a coherent oscillation between the momentum states [57]. After turning off the light grating diabatically, the atoms project into momentum states $|2n\hbar k_r\rangle$, where $n = 0, \pm1, \pm2, \ldots$ denotes the n^{th} order of the diffracted matter wave. In the weak-lattice limit, $U_0 \ll 4E_r$, only orders with $|n| \leq 1$ effectively participate in the coherent evolution, and the tune-out wavelength can be identified by decreasing population P_1 in the first-order diffraction peaks as U_0 approaches zero.

We employ a multipulse diffraction scheme to enhance the signal by constructive interference, as demonstrated in [30]. We pulse an optical lattice along one spatial dimension near the 741-nm transition with a detuning $\Delta = (\omega_L - \omega_0)/(2\pi)$, where ω_L is the laser frequency and ω_0 is the resonant frequency of the 741-nm transition. In the weak lattice limit, the oscillation period between $|0\rangle$ and $|\pm2\hbar k_r\rangle$ approaches $\tau = h/(4E_r) = 111$ μs for ^{162}Dy. As in [30], we use a square-wave sequence with n_p pulses since there is an n_p^2 enhancement in P_1 in the weakly diffracting limit ($n_p U_0 \ll 4E_r$) given by

$$P_1 = \frac{n_p^2 |U_0|^2}{32E_r^2}, \tag{1}$$

where the sign of U_0 can be determined by the sign of the detuning Δ. The pulse sequence has a 50% duty cycle with a period of 111 μs. Finally, we probe a range of Δ in search of the tune-out wavelength.

The quadratic scaling of P_1 with respect to n_p in Eq. (1) no longer holds after the diffracted peaks of atoms have sufficiently moved in space to lose coherence—and thus the ability to constructively interfere—with the main condensate. This coherence time limit from overlap loss sets the maximum pulse number where the quadratic scaling is valid. As shown in Fig. 2, the P_1 enhancement efficiency starts to drop below quadratic at $n_p = 10$, after which the atoms

Optics EXPRESS

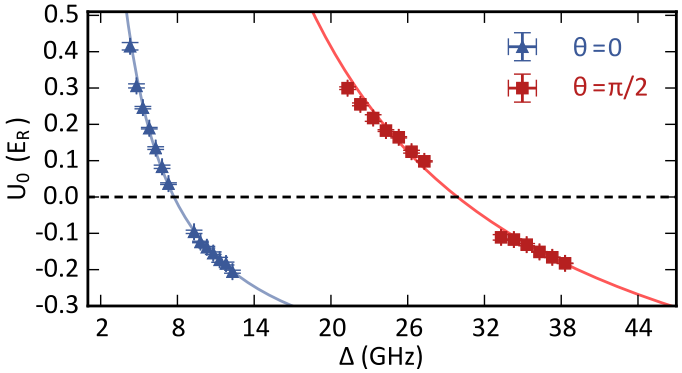

Fig. 3. Experimentally measured lattice depth versus detuning from the 741-nm transition for $\theta = 0$ (triangles) and $\theta = \pi/2$ (squares). Each point is an average of three measurements, and the lines are fits to the expected functional form of the Stark shift from Eq. (3). Error bars are 1σ standard error.

in $|\pm 2\hbar k_r\rangle$ have traveled 62% of the Thomas-Fermi radius. Therefore, for accurate light shift measurements, we employ a ten-pulse sequence to amplify P_1. The choice of n_p is appropriate for all Δ used in our measurements, because we operate in the weak-lattice limit, thus the coherence time only depends on k_r.

The tune-out wavelength is measured in terms of the detuning, denoted Δ_0, from the 741-nm transition frequency. We use a wavelength meter (HighFinesse WS/6 200) to monitor the frequency of the lattice beam derived from a Ti:Sapphire laser. We calibrate the wavelength meter against a frequency-stabilized 741-nm diode cooling laser with a <10 kHz/h drift rate [8] via a beat note setup. While simultaneously monitoring the frequency of the lattice beam and the cooling laser on the wavelength meter, we combine beams of both lasers onto a high-speed photodetector (Electro-Optics Technology ET-4000). We then compare the beat signal frequency, measured up to ±8 GHz, to the frequency difference given by the wavelength meter. Applying this calibration beyond the range of ±8 GHz yields an uncertainty of 10 MHz in the frequency measurement.

We prepare Bose-Einstein condensates (BECs) of ^{162}Dy using methods described in [12]. The resulting trap frequencies are $\left[f_x, f_y, f_z\right] = [62(2), 32(4), 113(2)]$ Hz, where gravity is along $\hat{z}$. We initiate KD diffraction with a nearly pure BEC of 5×10^4 atoms in the maximally stretched ground state $|J = 8, m_J = -8\rangle$. As illustrated in Fig. 1, the 1D lattice is formed along $\hat{x} + \hat{y}$ by retroreflecting a 0.20(2)-W collimated beam with a diameter of 950 μm. The light field polarization is kept linear along $\hat{z}$, purified by a polarizing beam splitter. Therefore, any anisotropy in Δ_0 should be attributed to the tensor light shift since the vector light shift is identially zero for linearly polarized light (see second term in Eq. (2) below). To probe the anisotropy in Δ_0, we perform the measurement at two different field orientations $\hat{z}$ and $\hat{x} - \hat{y}$, both at a field magnitude of 1.580(5) G, to realize $\theta = 0$ and $\theta = \pi/2$ in Eq. (2). We note that this field is away from any Feshbach resonances [58].

Optics EXPRESS

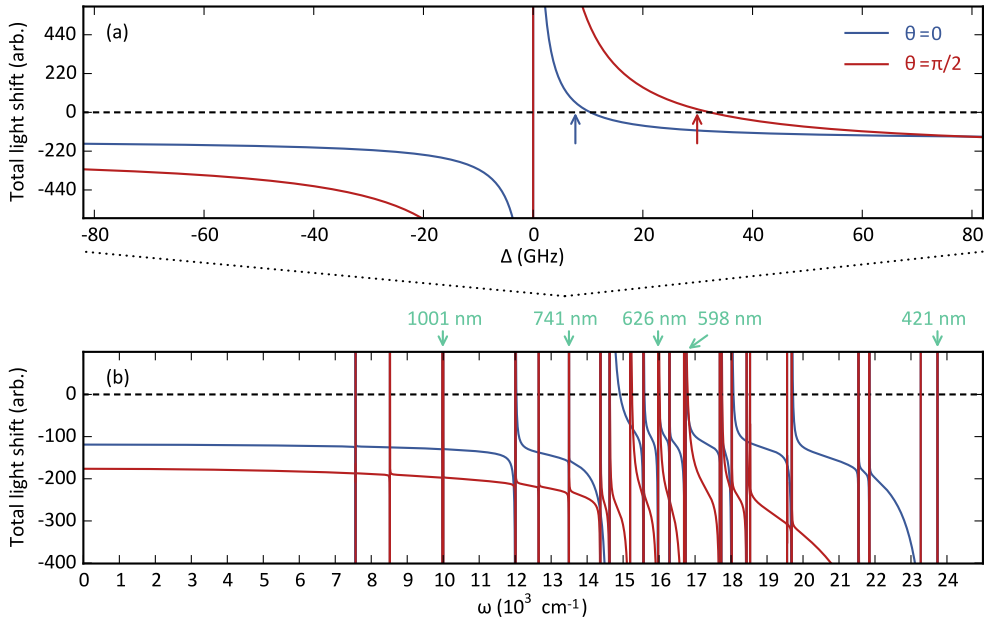

Fig. 4. (a) Calculated total light shift (arbitrary unit) versus detuning from the 741-nm line for both $\theta = 0$ and $\theta = \pi/2$. The arrows indicate the positions of the measured Δ_0 points. The 160-GHz window corresponds to 5 cm^{-1}. (b) Calculated total light shift (arbitrary unit) for both polarizations between laser frequencies (wavelengths) DC and 24,000 cm^{-1} (417 nm). The cycling transitions ($J \rightarrow J' = J + 1$) are indicated in turquoise [4, 59]. The large anisotropy at far-off resonant frequencies is likely a result of incomplete knowledge of atomic transition data; see main text for details.

3. Stark shift calculation

For a single transition from the ground state $|F, m_F\rangle$ to an excited state $|F', m_{F'}\rangle$, the light shift of the ground state with an applied optical field of angular frequency ω is given by

$$\Delta U_{(F,m_F)} = -\alpha^{(0)}|\vec{E}_0^{(+)}|^2 - \alpha^{(1)}\left[i\vec{E}_0^{(-)} \times \vec{E}_0^{(+)}\right]_z \frac{m_F}{F} - \alpha^{(2)}|\vec{E}_0^{(+)}|^2 \left(\frac{3\cos^2\theta - 1}{2}\right)\left[\frac{3m_F^2 - F(F+1)}{F(2F-1)}\right],$$

$$\alpha^{(0)} = \frac{2\omega_{FF'}|\langle F||\vec{d}||F'\rangle|^2}{3\hbar(2F+1)(\omega_{FF'}^2 - \omega^2)},$$

$$\alpha^{(1)} = (-1)^{F+F'+1}\sqrt{\frac{6F}{(F+1)(2F+1)}}\begin{Bmatrix} 1 & 1 & 1 \\ F & F & F' \end{Bmatrix}\frac{\omega|\langle F||\vec{d}||F'\rangle|^2}{\hbar(\omega_{FF'}^2 - \omega^2)},$$

$$\alpha^{(2)} = (-1)^{F+F'}\sqrt{\frac{40F(2F-1)}{3(F+1)(2F+1)(2F+3)}}\begin{Bmatrix} 1 & 1 & 2 \\ F & F & F' \end{Bmatrix}\frac{\omega_{FF'}|\langle F||\vec{d}||F'\rangle|^2}{\hbar(\omega_{FF'}^2 - \omega^2)}, \quad (2)$$

where $\vec{E}_0^{(+)}$ and $\vec{E}_0^{(-)}$ are the rotating and counter-rotating part of the optical field; θ is the angle between its polarization and the quantization axis set by the magnetic field; $\omega_{FF'}$ is the transition angular frequency; $\alpha^{(0)}$, $\alpha^{(1)}$, and $\alpha^{(2)}$ are the scalar, vector and tensor polarizabilities; and $|\langle F||\vec{d}||F'\rangle|^2$ is the reduced dipole matrix element [60–63]. As in [47], we add a constant offset of $\alpha' = 94.27$ atomic units (a.u.) to the calculated scalar polarizability to match the latest

Optics EXPRESS

experimentally measured scalar polarizability at DC for ^{162}Dy [64]. A similar correction for the tensor polarizability may be necessary but is yet unmeasured. From Eq. (2), we note that while the scalar part preserves spherical symmetry, the vector light shift is dependent on the cross product of the rotating and counter-rotating electric fields and therefore vanishes if the polarization is linear. The tensor term also breaks spherical symmetry with a θ-dependence such that it is maximized at $\theta = 0$ and minimized at $\theta = \pi/2$.

The light shift of alkali atoms at large detuning is due solely to the scalar shift and is spherically symmetric. For these atoms, when the laser detuning is large compared to the hyperfine splitting of the excited state, the hyperfine levels become effectively degenerate and the optical field interacts directly with the fine-structure transition. That is, the hyperfine transition $F \rightarrow F'$ is replaced by the fine-structure transition $J \rightarrow J'$, $\omega_{FF'}$ is replaced by $\omega_{JJ'}$, and the polarizabilities can be directly expressed by the fine-structure dipole matrix elements. For alkali atoms in the ground state $|J = 1/2, L = 0\rangle$, the tensor polarizability $\alpha^{(2)}$ vanishes at large detuning, and the vector polarizability $\alpha^{(1)}$ is canceled by opposite contributions from the D_1 and D_2 lines [34, 60, 61].

This spherical symmetry does not hold for Dy from the ground state $|J = 8, L = 6\rangle$ due to its large orbital angular momentum (bosonic Dy has zero nuclear spin). For example, the tensor polarizability $\alpha^{(2)}_{741}$ for the 741-nm $J = 8 \rightarrow J' = 9$ transition does not vanish like the alkali $J = 1/2 \rightarrow J'$ transitions. On the contrary, it is on the same order of magnitude as the scalar polarizability $\alpha^{(0)}_{741}$ for all detunings ($\alpha^{(2)}_{741} \approx -0.7\alpha^{(0)}_{741}$).

4. Results

We measure P_1 and determine U_0 using Eq. (1). Fig. 3 shows the measured U_0 with respect to the detuning Δ from the 741-nm resonance for both $\theta = 0$ and $\theta = \pi/2$. We find that P_1 decreases as the laser is detuned further on the blue side of the 741-nm transition. Eventually, P_1 drops below the noise floor in our absorption image. As we further increase Δ, we observe a revival in P_1, indicating a sign change in the total light shift. We observe a clear polarization-dependence in Δ_0, which differs by more than 20 GHz for the two polarizations.

We perform a least-squares fit to the data to quantitatively determine Δ_0, using

$$U_0 = A + \frac{B}{\Delta} \tag{3}$$

as the fit model, where A and B are free parameters. Due to the large number of dysprosium lines, it is intractable at present for us to use the exact analytical form of the total light shift as the fit function. However, since the detuning from all lines other than the 741-nm transition is large, we simply treat the contribution from these other lines as a constant background. The fitted curves cross zero at $\Delta_0(\theta = 0) = 7.7(1)$ GHz and $\Delta_0(\theta = \pi/2) = 29.9(1)$ GHz, resulting in a 22.2-GHz polarization-dependent anisotropy in Δ_0. The ratio of this anisotropy to the detuning from the 741-nm resonance is nearly five orders of magnitude larger than ratio of Rb's tune-out wavelength anisotropy (~44 MHz) to the detuning (~10 nm) from the D_1 and D_2 lines [34].

We also compare the measured Δ_0 values to the calculated Stark shift in Fig. 4. We compute the total Stark shift using the formalism presented in Section 3. To account for all the known transitions of dysprosium, we sum over Eq. (2) for the 26 lines documented in [47], replacing the listed theoretical matrix elements with experimentally measured values when possible (e.g., the 741-nm transition [59]). The calculated values—$\Delta^{\text{th}}_0(\theta = 0) = 10.4$ GHz and $\Delta^{\text{th}}_0(\theta = \pi/2) = 32.2$ GHz—differ from the measured values by 26% and 7%, respectively.

Furthermore, while [59] reports an experimentally measured linewidth of 1.78(2) kHz for the 741-nm excited state, we extract a linewidth by setting the reduced matrix element for the 741-nm transition μ_{741} as the free parameter and minimize the error function

$$E(\mu_{741}) = \sum_{\theta=0,\pi/2} \left[\Delta^{\text{th}}_0(\theta) - \Delta_0(\theta)\right]^2_{\mu_{741}}, \tag{4}$$

Optics EXPRESS

which is the discrepancy between the calculated tune-out wavelengths Δ_0^{th}, evaluated at μ_{741}, and the experimental values Δ_0 at $\theta = 0$ and $\theta = \pi/2$. Despite the lack of the comprehensive measurements of all matrix elements of dysprosium [47], we obtain 1.62(1) kHz, which differs from the experimental value reported in [59] by 10%.

Figure 4 suggests that the total light shift at $\theta = 0$ and $\theta = \pi/2$ should differ by around 50% near 1064 nm (9,398 cm^{-1}), a common wavelength for optical dipole traps, and the one employed here. To explore this, we measure the trap frequency along $\hat{z}$ for fields along $\hat{z}$ and $\hat{x}$, which correspond to $\theta = 0$ and $\theta = \pi/2$, respectively. Nevertheless, we find that the trap shape is isotropic to within 3%, in contradiction to the prediction. This isotropy has also been predicted in the optical trapping of erbium, another lanthanide atom, at 1064 nm using 1284 lines, 33 of which have been observed experimentally [49]. A similar calculation has been recently conducted for dysprosium [48]. In summary, a more complete knowledge of the dysprosium atomic spectrum is required to improve the agreement between theoretically predicted and experimentally measured tune-out wavelengths, and to properly account for the far-off-resonance regime.

5. Conclusions

The measurement of the tune-out wavelengths for ^{162}Dy near the narrow 741-nm transition has been presented, along with a calculation that reproduces these wavelengths within a few GHz. As also predicted, we observe an anisotropy in the tune-out wavelength as a function of the relative angle between the optical field polarization and the quantization axis.

While this work focuses on the tune-out wavelengths of ^{162}Dy, those of the other bosonic isotopes of Dy are related to ^{162}Dy's by the isotope shifts, 1214(3) MHz and -1338(6) MHz for ^{164}Dy and ^{160}Dy, respectively [59], since nuclear effects play little role within the resolution of our measurement and bosonic Dy is $I = 0$. However, the wavelengths of the fermionic isotopes cannot be accurately determined with this data since those isotopes do possess hyperfine structure on the GHz scale. Analogous measurements using Kapitza-Dirac diffraction for (near) degenerate fermions is much more challenging due to the intrinsically larger momentum spread.

Funding

We acknowledge support from the AFOSR and NSF. Y.T. acknowledges partial support from the Stanford Graduate Fellowship.

Acknowledgments

We thank V. Vaidya for valuable discussions.